

An entangled-light-emitting diode

C. L. Salter^{1,2}, R. M. Stevenson¹, I. Farrer², C. A. Nicoll², D. A. Ritchie² & A. J. Shields¹

By
Yasaman Soudagar

Aug. 11, 2010

An optical quantum computer, powerful enough to solve problems so far intractable using conventional digital logic, requires a large number of entangled photons^{1,2}. At present, entangled-light sources are optically driven with lasers³⁻⁷, which are impractical for quantum computing owing to the bulk and complexity of the optics required for large-scale applications. Parametric down-conversion is the most widely used source of entangled light, and has been used to implement non-destructive quantum logic gates^{8,9}. However, these sources are Poissonian^{4,5} and probabilistically emit zero or multiple entangled photon pairs in most cycles, fundamentally limiting the success probability of quantum computational operations. These complications can be overcome by using an electrically driven on-demand source of entangled photon pairs¹⁰, but so far such a source has not been produced. Here we report the realization of an electrically driven source of entangled photon pairs, consisting of a quantum dot embedded in a semiconductor light-emitting diode (LED) structure. We show that the device emits entangled photon pairs under d.c. and a.c. injection, the latter achieving an entanglement fidelity of up to 0.82. Entangled light with such high fidelity is sufficient for application in quantum relays¹¹, in core components of quantum computing such as teleportation¹²⁻¹⁴, and in entanglement swapping^{15,16}. The a.c. operation of the entangled-light-emitting diode (ELED) indicates its potential function as an on-demand source without the need for a complicated laser driving system; consequently, the ELED is at present the best source on which to base future scalable quantum information applications¹⁷.

Outline:

- Biexcitons:

How do they give rise to polarization entanglement?

- Fabrication:

1. What should be taken into account

2. Process

- Experimental setup

- Results and Analysis

Biexciton and Polarization Entanglement

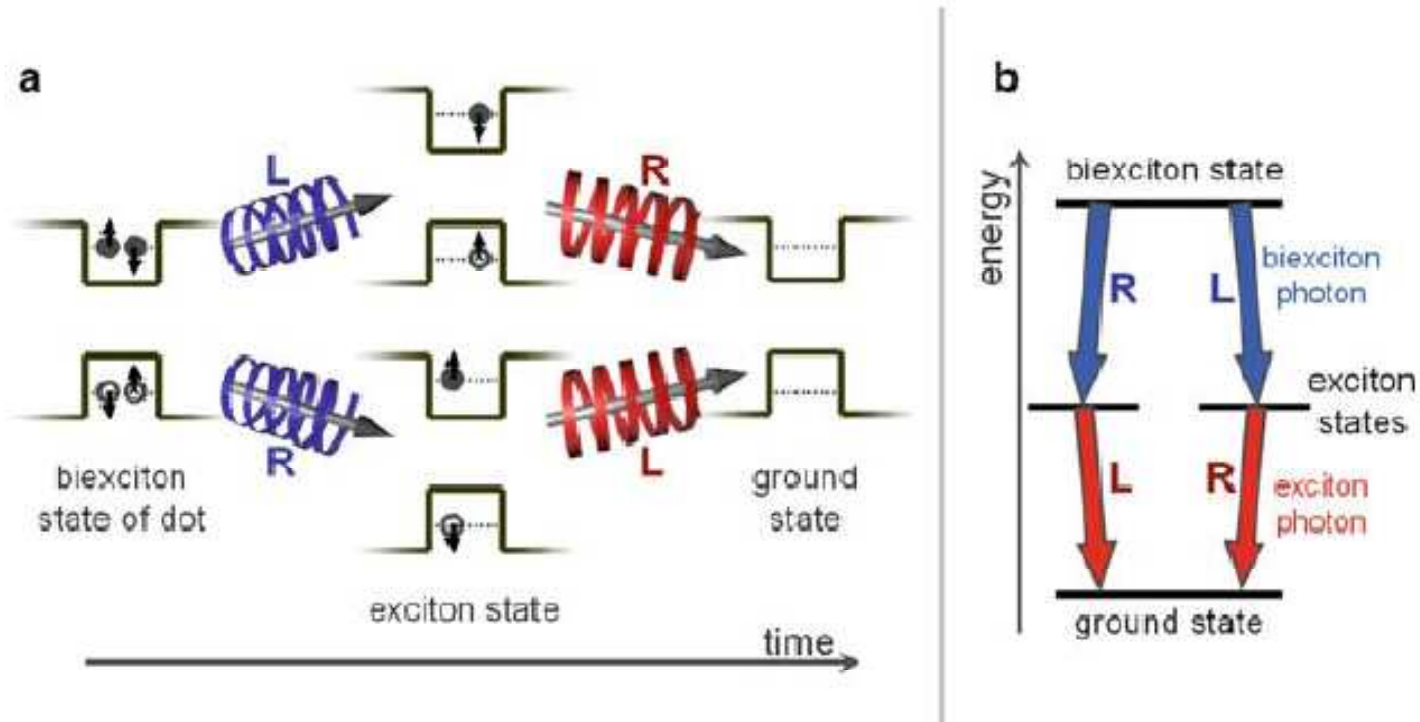


Fig. 7.1. (a) An illustration of the radiative decay process of the biexciton state from a single quantum dot. Recombination of electrons and holes results in the emission of a pair of photons via one of two intermediate exciton states. Ideally the emitted photons are right (R) and left (L) circularly polarised. (b) The same two-photon emission process in a simple energy level diagram. The biexciton photons are typically more energetic than the exciton photons

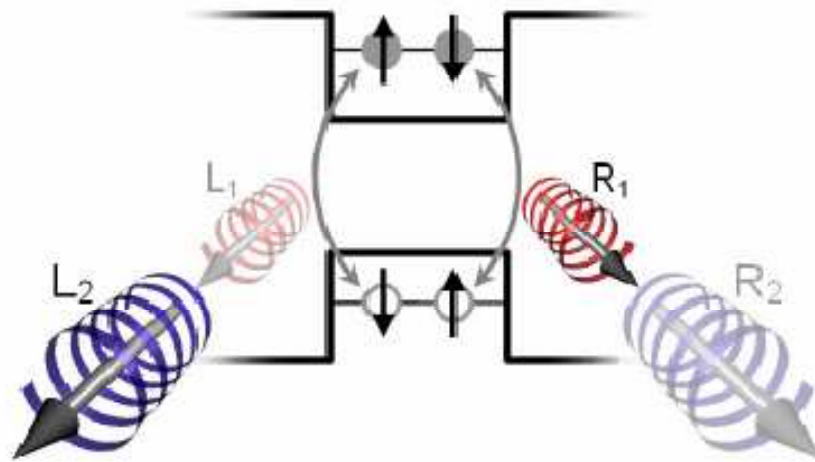


Figure 1. The two-photon biexciton decay process of a quantum dot with no bright exciton splitting. Recombination of a spin-up (-down) electron and a spin-down (-up) hole generates a left (right) hand circularly polarised photon. Since it is impossible to predict which photon will be emitted first, the emission is expected in the entangled state $(|L_1R_2\rangle + |R_1L_2\rangle)/\sqrt{2}$. Subscripts denote the order of emission of the left, L and right, R polarised photons.

Fine Structure Splitting in Biexcitons

A semiconductor source of triggered entangled photon pairs

R. M. Stevenson¹, R. J. Young^{1,2}, P. Atkinson², K. Cooper², D. A. Ritchie² & A. J. Shields¹

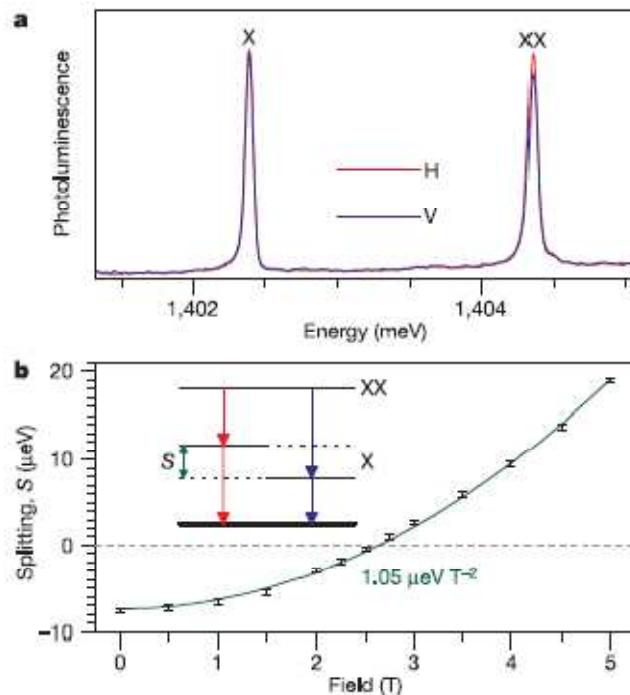


Figure 1 | Polarized photoluminescence spectra from single quantum dots.
a, Vertically (blue) and horizontally (red) polarized photoluminescence for a single quantum dot with small polarization splitting. The features correspond to emission by the exciton (X) and biexciton (XX) state.
b, Polarization splitting, S , as a function of in-plane magnetic field for a single dot with 'inverted' S at 0 T. The green line shows a quadratic fit to the data with a coefficient of $1.05 \mu\text{eV T}^{-2}$. Inset shows the level diagram of the radiative decay of the biexciton state. The competing two photon decay paths are distinguished only by the polarization of the photons, indicated by the arrow colour, and the splitting, S , of the intermediate exciton level. Error bars span two standard deviations from the fitted line.

$$|\Psi\rangle = (|H_{XX}H_X\rangle + e^{i\delta_1\tau/\hbar}|V_{XX}V_X\rangle)/\sqrt{2}.$$

Delta 1 = S → the splitting

Integration over T destroys the Entanglement as it mixes the phases between Two terms, unless delta1 or the splitting is very Small.

How to get small splitting:

Typically an energetic splitting (S) between the two intermediate exciton states provides such information, though there has been a significant effort made by a number of groups worldwide to reduce the exciton level splitting.

These include

- * the simple selection of dots with small splitting [6, 10, 11],
- * rapid thermal annealing of samples containing quantum dots [10, 12, 13],
- * applying an in-plane electric [14, 15], magnetic [16, 17] or strain [18] field,
- * and post-emission spectral filtering of the photons [5].

**Young, R. J. et al. Bell-inequality violation with a triggered photon-pair source.
Phys. Rev. Lett. 102, 030406 (2009)**

Device and its Fabrication

We fabricated the ELED from a p-i-n heterostructure grown by molecular beam epitaxy. It comprises fourteen GaAs/Al_{0.98}Ga_{0.02}As distributed-Bragg-reflector repeats below, and two above, an InAs quantum dot layer formed at the centre of a GaAs microcavity. We used standard photolithography and wet etching techniques to fabricate a diode with an area of $\sim 360 \mu\text{m} \times 360 \mu\text{m}$. One hundred $\sim 2\text{-}\mu\text{m}$ -diameter apertures in an aluminium shadow mask on the top of the device isolated emission from individual quantum dots. Typically, one quantum dot per device yielded a small enough fine structure splitting for strong entanglement. The number of useful dots per device could be increased by growth on (111)B GaAs substrates³⁰.

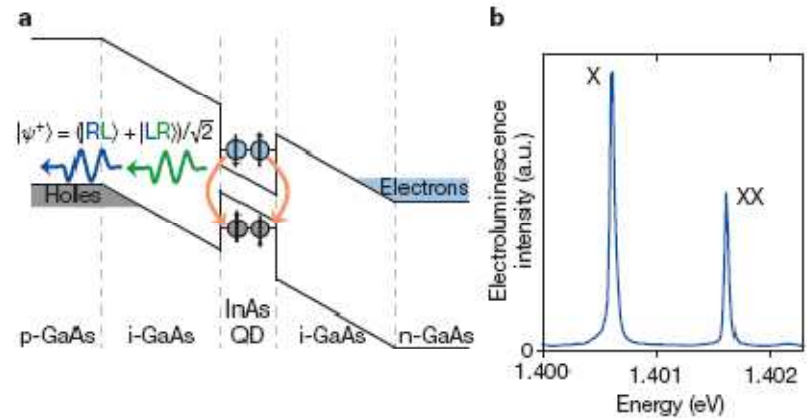
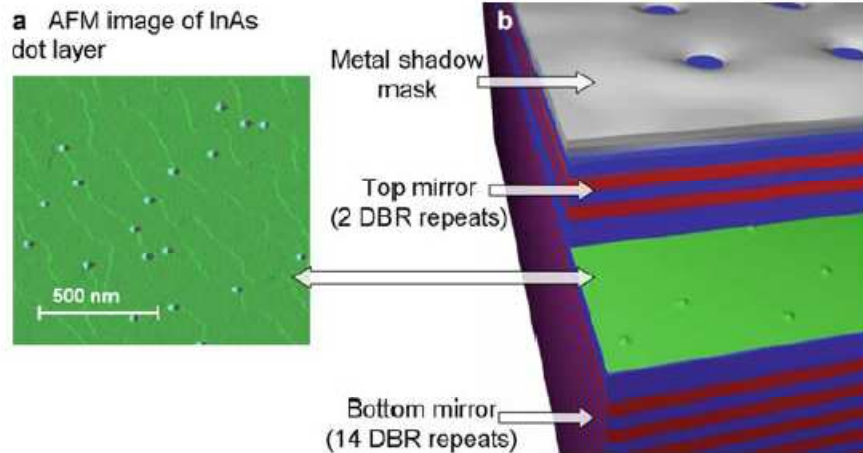


Figure 1 | Device design and operation. **a**, Schematic of the active region of the ELED, showing the emission of a polarization entangled photon pair through the biexciton cascade. The different regions of the heterostructure are labelled. Here the diode is in its 'off' state, just after non-resonant electrical injection of two electrons (blue circles) and two holes (grey circles) into the quantum dot (QD). The orange arrows represent recombination of the carriers and the blue and green arrows represent the subsequent entangled photon pair. **b**, Electroluminescence spectrum of the quantum dot investigated in this report using d.c. electrical injection with a current density of $31 \text{ nA } \mu\text{m}^{-2}$. a.u., arbitrary units.

Crucial features of design

1. Cavity is double resonant: thick
2. Large intrinsic region stops electrons from negative region to tunnel into the biexciton after the first photon gets out
3. Make sure the energy of emitted photons is ~ 1.4 eV. This ensures small fine structure splitting.

Molecular Beam Epitaxy

MBE

Movie time!

Experimental parameters

- D.C. current density of 31 nAum^{-2} , 2ns coincidence window:

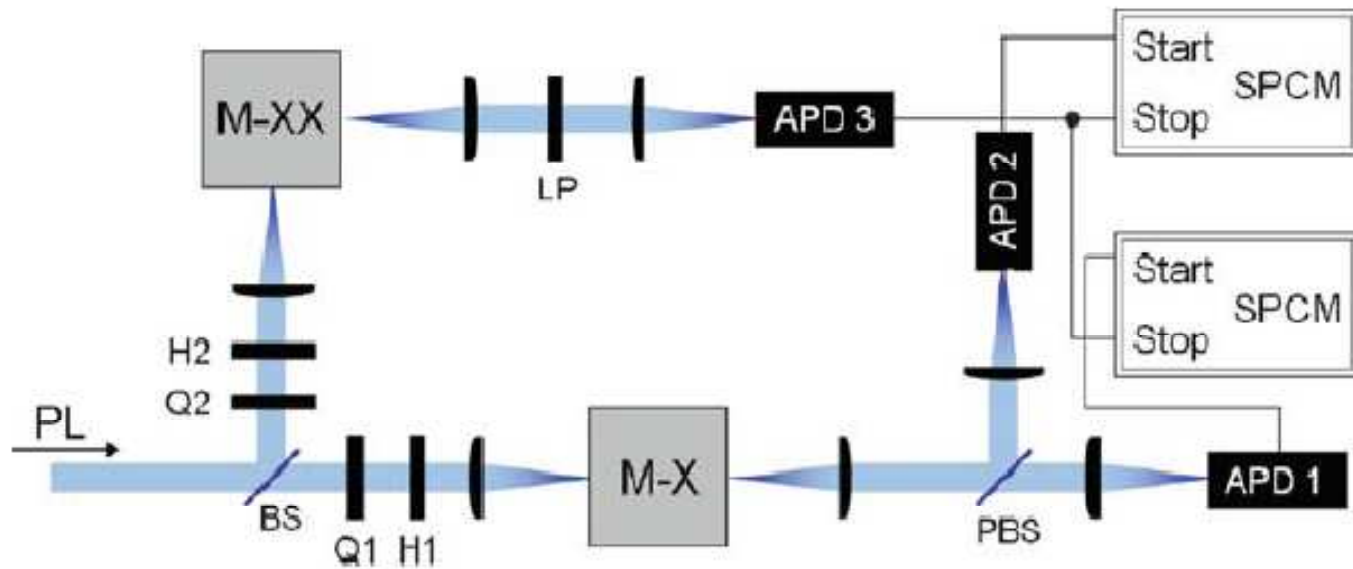
Entangled pair detection rate of $\sim 9,900$ per hour

- AC mode 4.5V pulse, width 300ps, superimposed on a 2.0V DC signal:

Entangled pair detection rate was ~ 940 per hour. Prob of emitting and entangled pair per cycle is 3%.

Electroluminescence was collected using a microscope objective lens, dispersed using a grating spectrometer and recorded using a charge-coupled device. Polarization-dependent measurements allowed measurement of the fine-structure splitting²³ and identification of suitable dots.

Exp sketch



What to measure?

Density Matrix to be theoretically reconstructed:

$$\underline{\underline{\rho}} = \begin{pmatrix} \rho_{11} & \rho_{12} & \rho_{13} & \rho_{14} \\ \rho_{12}^* & \rho_{22} & \rho_{23} & \rho_{24} \\ \rho_{13}^* & \rho_{23}^* & \rho_{33} & \rho_{34} \\ \rho_{14}^* & \rho_{24}^* & \rho_{34}^* & \rho_{44} \end{pmatrix}$$

But it seems that it cannot be done probably due to low count rate

The correlation coefficient:

$$E_{\alpha\beta} = I(a, b) + I(\bar{a}, \bar{b}) - I(a, \bar{b}) - I(\bar{a}, b)$$

where $I(a, b)$ is the normalised intensity (i.e. probability) of detection of the first and second photon with polarisations a and b , which together with the orthogonal polarisations \bar{a} and \bar{b} form the polarisation bases α and β . Values of $E = 0, 1$ and -1 indicate no correlation, maximum correlation, and maximum anti-correlation respectively.

Degree of polarization:

Ratio of the intensity of polarized light to the total intensity

Component for rectilinear bases for one photon:

$$P_{r1} = I(H, H) + I(H, V) - I(V, H) - I(V, V)$$

Density Matrix in terms of correlations and degrees of polarization

$$\underline{\underline{\rho}} = \frac{1}{4} \begin{pmatrix} 1 + E_{rr} + P_{r1} + P_{r2} & E_{rd} + P_{d2} & E_{dr} + P_{d1} & E_{dd} - E_{cc} \\ E_{rd} + P_{d2} & 1 - E_{rr} + P_{r1} - P_{r2} & E_{dd} + E_{cc} & -E_{dr} + P_{d1} \\ E_{dr} + P_{d1} & E_{dd} + E_{cc} & 1 - E_{rr} - P_{r1} + P_{r2} & -E_{rd} + P_{d2} \\ E_{dd} - E_{cc} & -E_{dr} + P_{d1} & -E_{rd} + P_{d2} & 1 + E_{rr} - P_{r1} - P_{r2} \end{pmatrix} \\
 + \frac{i}{4} \begin{pmatrix} 0 & -E_{rc} - P_{c2} & -E_{cr} - P_{c1} & -E_{cd} - E_{dc} \\ E_{rc} + P_{c2} & 0 & -E_{cd} + E_{dc} & E_{cr} - P_{c1} \\ E_{cr} + P_{c1} & E_{cd} - E_{dc} & 0 & E_{rc} - P_{c2} \\ E_{cd} + E_{dc} & -E_{cr} + P_{c1} & -E_{rc} + P_{c2} & 0 \end{pmatrix} \quad (7.1)$$

Fidelity

$$f^+ = \langle \psi^+ | \underline{\underline{\rho}} | \psi^+ \rangle$$

$$f^+ = \langle \psi^+ | \underline{\underline{\rho}} | \psi^+ \rangle = (\rho_{11} + \rho_{44})/2 + \text{Re}\{\rho_{14}\}$$

$$f^+ = (E_{rr} + E_{dd} - E_{cc} + 1)/4$$

For unpolarized light:

$$\hat{E}_{\alpha\beta} = I(a, b) - I(a, \bar{b})$$

In the language of the paper:

$$\hat{E}_{\alpha\beta} = I(a, b) - I(a, \bar{b}) \longrightarrow C(\tau) = \frac{g_{XX,X}^{(2)}(\tau) - g_{XX,\bar{X}}^{(2)}(\tau)}{g_{XX,X}^{(2)}(\tau) + g_{XX,\bar{X}}^{(2)}(\tau)}$$

$$f^+ = \frac{1}{4}(1 + C_{\text{rectilinear}} + C_{\text{diagonal}} - C_{\text{circular}})$$

Bell parameters: CHSH inequality

$$S = E(\alpha, \beta) - E(\alpha', \beta) + E(\alpha, \beta') + E(\alpha', \beta') \leq 2$$

$$S_{\text{RD}} = \sqrt{2}(C_{\text{rectilinear}} + C_{\text{diagonal}}) \leq 2$$

$$S_{\text{DC}} = \sqrt{2}(C_{\text{diagonal}} - C_{\text{circular}}) \leq 2$$

$$S_{\text{RC}} = \sqrt{2}(C_{\text{rectilinear}} - C_{\text{circular}}) \leq 2$$

Results:

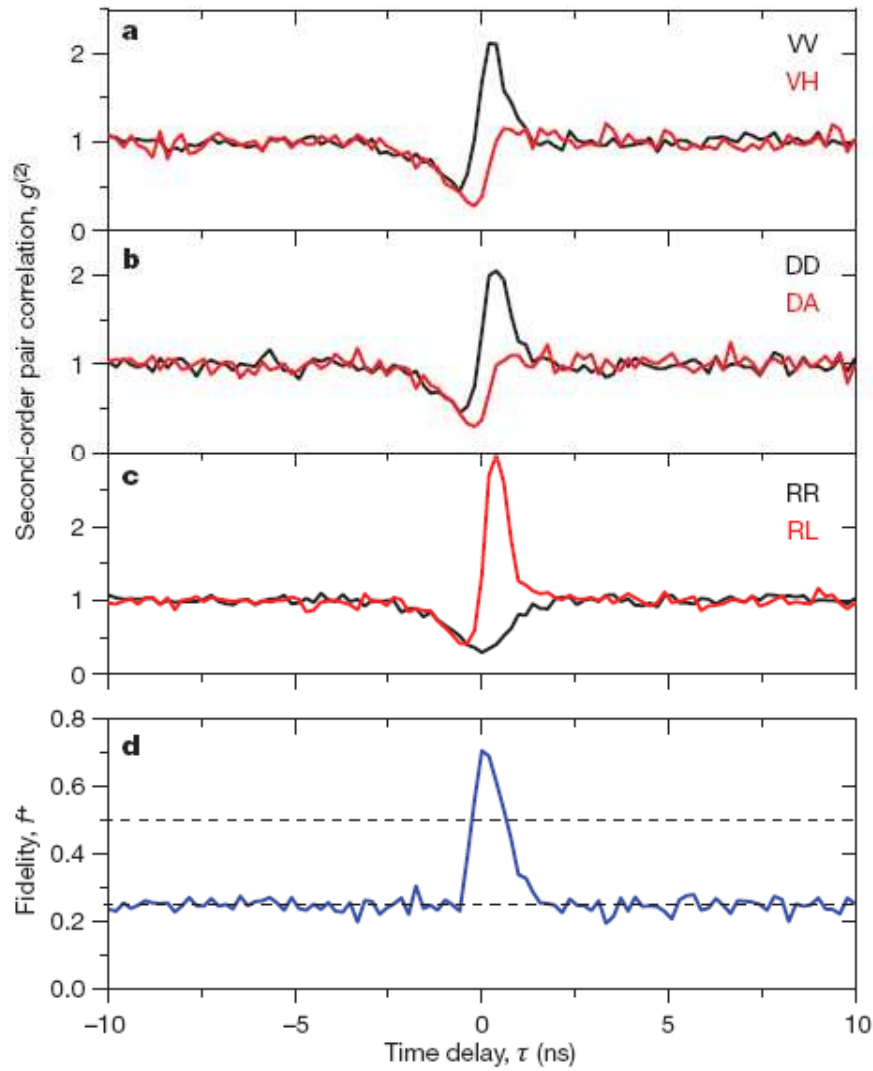
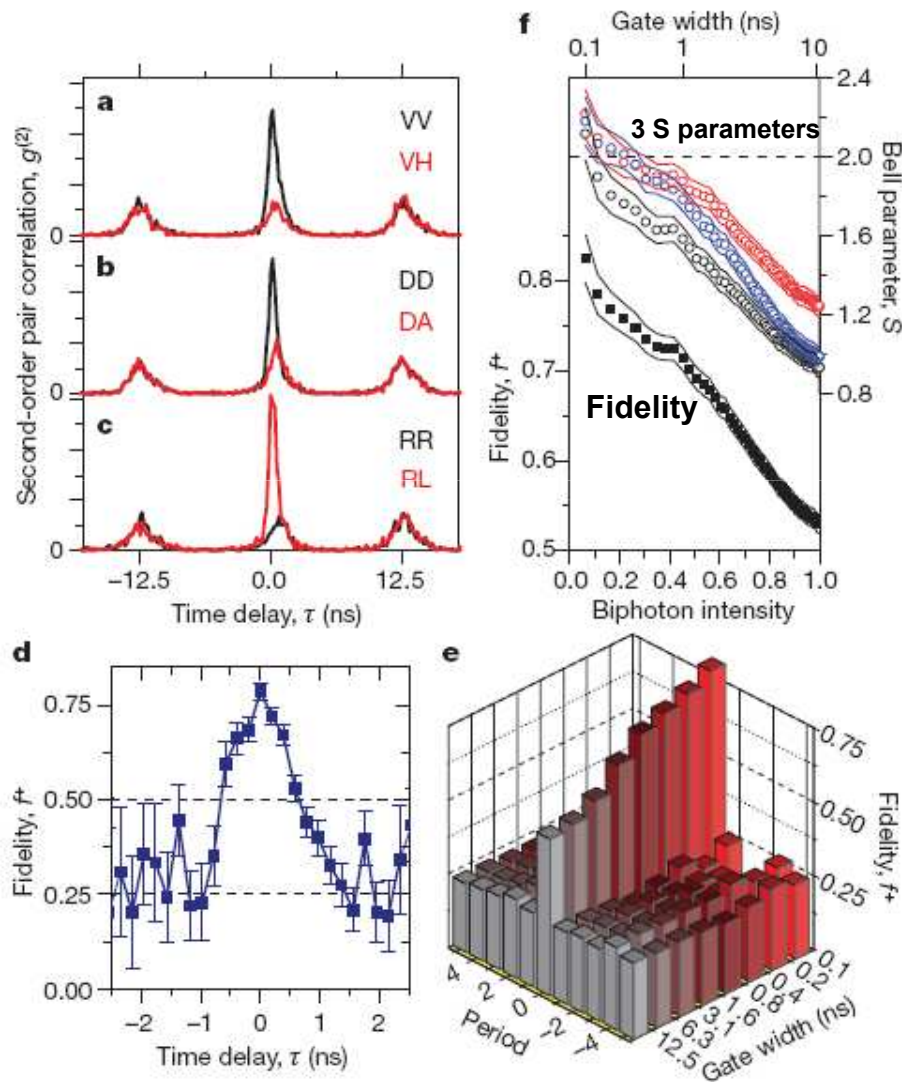


Figure 2 | Polarized pair-correlation results from d.c. electrical injection into the ELED. The current density is $31 \text{ nA } \mu\text{m}^{-2}$. **a–c**, $g_{XX,X}^{(2)}(\tau)$ and $g_{XX,\bar{X}}^{(2)}(\tau)$ measured in the rectilinear (**a**), diagonal (**b**) and circular (**c**) bases with a time resolution of 0.2 ns. Labels denote the polarizations of the first (XX) and second (X) photons (in that order) as vertical (V), horizontal (H), diagonal (D), anti-diagonal (A), right-handed circular (R) and left-handed circular (L). Correlations measured for photons of the same polarization ($g_{XX,X}^{(2)}(\tau)$) are shown in black and those measured for photons of orthogonal polarizations ($g_{XX,\bar{X}}^{(2)}(\tau)$) are shown in red. **d**, Fidelity, f^+ , measured as a function of time delay, τ . The dashed lines represent the classical threshold fidelity, of 0.5, and the uncorrelated-light fidelity, of 0.25.

bases²⁰, as described in Methods Summary. The peak at $\tau = 0$ gives a maximum d.c. fidelity of $f^+ = 0.707 \pm 0.023$, without any background light subtraction. This exceeds by 9 s.d. the threshold, of 0.5, for a

Results



shows the results of polarized-photon-pair correlation experiments conducted when the device was pulsed with an alternating current at a repetition rate of 80 MHz (pulse period, 12.5 ns). As for the d.c. case

Figure 3 | Polarized pair-correlation results from a.c. electrical injection into the ELED. **a-c,** $g_{XX,X}^{(2)}(\tau)$ and $g_{XX,\bar{X}}^{(2)}(\tau)$ measured in the rectilinear (a), diagonal (b) and circular (c) polarization bases with a time resolution of 0.2 ns. **d,** Corresponding fidelity about zero time delay. The dashed lines represent the classical threshold fidelity, of 0.5, and the uncorrelated-light fidelity, of 0.25. Error bars, 1 s.d. **e,** Fidelity as a function of gate width for the 11 central pulse periods. **f,** Fidelity at $\tau = 0$ (filled squares) and the Bell parameters (open circles: black, S_{RD} ; blue, S_{DC} ; red, S_{RC}) as functions of the proportion of the total biphoton intensity that is analysed. The biphoton intensity is varied by changing the gate width (top axis). Solid lines indicate 1-s.d. error envelopes. Reduced biphoton intensity (f) and non-zero delay (d) diminish the measured coincidences and thus increase error due to Poissonian counting statistics. This also explains the fluctuations in fidelity about 0.25 for the non-zero periods in e at very low gate widths.

proportion of background light. The lowest gate width, of 0.1 ns, gives the maximum a.c. fidelity, $f^+ = 0.826 \pm 0.027$.

Results and conclusion:

in all three polarization bases. At the lowest gate width (0.1 ns), we find that $S_{RD} = 2.12 \pm 0.13$, $S_{DC} = 2.18 \pm 0.12$ and $S_{RC} = 2.22 \pm 0.12$. The

We have eliminated the need for large and complicated laser driving systems in future quantum information applications by demonstrating high-fidelity entangled-light emission triggered from an LED. Entangled photon pairs with such high fidelity are sufficient for teleportation¹²⁻¹⁴ and entanglement swapping^{15,16}, which are important components in a quantum computer. Improvements to the ELED such as reducing the background light emission^{25,29} and increasing the speed of the device to minimize re-excitation during pulsing could be made to increase the fidelity further, and eventually to realize electrically operated fault-tolerant quantum computing.